RESEARCH ARTICLE

Journal Section

Simple formulas for pseudoposition for electrical resistivity and IP in vertical boreholes based on mean positions of the sensistivity

S.L. Butler PhD[1*]

[1]S.L. Butler Dept. of Geological Sciences, University of Saskatchewan

Correspondence
S.L. Butler, Dept. of Geological Sciences, University of Saskatchewan, Saskatoon, Saskatchewan, S7K 2Y6, Canada
Email: sam.butler@usask.ca

Funding information
Natural Sciences and Engineering Research Council of Canada Discovery Grant

The electrical conductivity method in boreholes has been applied for exploration as well as engineering and environmental investigations. The simplest deployment involves placing electrodes at varying heights within a single borehole. Borehole surveys differ from surface surveys using colinear arrays in that the ground surface is in the line of the electrodes and so it influences the measured potential in the ground differently. Multiple electrodes can be deployed on a single multichannel cable resulting in measurements from nonstandard array configurations. The choice of the plot point for pseudosections can be difficult for these nonstandard arrays. The mean of the sensitivity function of a constant resistivity half space has been shown to yield simple and useful formulas for pseudopositions for four electrode surface arrays. In this contribution, I first derive the sensitivity function for electrodes in a vertical borehole and then calculate the vertical and horizontal sensitivity functions. I then derive simple formulas for the vertical and horizontal positions of the mean of the sensitivity function for electrodes in a vertical borehole. Pseudosections for synthetic data are shown to be more easily interpretable than pseudosections plotted using averages of the electrode positions. The simple formulas will be useful for plotting pseudosections for initial data visualization and for survey plan-

ning.

KEYWORDS
resistivity, borehole, pseudoposition

1 | INTRODUCTION

The electrical resistivity method is one of the most widely used methods in geophysics (*Reynolds*, 2011; *Loke et al.*, 2013; *Bhattacharya and Shalivahan*, 2016). The method has been widely deployed on the surface, however, surveys have also been deployed in boreholes (*Daniels and Van Dyck*, 1984; *Spies*,1996) for exploration (*Daniels and Van Dyck*, 1984; *Qian et al.*, 2007; *Ali et al.*, 2020) as well as for engineering applications (*Denis et al.*, 2002).

Electrodes can be deployed in boreholes in a number of different configurations including Vertical Resistivity Profiles (VRP) in which all of the electrodes are placed in a single vertical borehole, borehole to borehole configurations and borehole to surface configurations (*Daniels and Van Dyck*, 1984; Ali et al., 2020). While inversion of resistivity data is now always the final product of a resistivity survey, plotting of pseudosections of both resistivity and induced polarization (IP) data remains useful as it serves as a preliminary visualization of the data. Also, apparent resistivity pseudosections of the field-measured data and data calculated from forward models using the final inverted ground resistivity are typically compared in order to gauge the quality of the inversion. Additionally, knowledge of plot points in pseudosections, or pseudopositions, for a given array configuration is useful for survey planning as they give an idea of the region of investigation.

The pseudopositions for surface arrays have typically been determined either using rules of thumb or considering the median of the sensitivity function for an infinite half space based on the work of *Roy and Apparoa* (1971) and *Edwards* (1977). For symmetrical linear surface arrays such as pole-pole, Wenner, Schlumberger and dipole-dipole arrays, the horizontal pseudoposition is usually taken to be at the mid-point of the array. Many modern aquisition systems collect data on multiple channels simultaneously for a single current injection pair, in which case many of the arrays will be asymmetric and the horizontal pseudoposition cannot be determined from a midpoint. Similarly for 3D data, the horizontal pseudoposition may not be obvious. *Butler* (2017) showed that the mean or average horizontal position of the horizontal sensitivity function for a constant resistivity half space, first derived by *Banerjee and Pal* (1986), yields a simple mathematical expression and that the use of the average horizontal position as the horizontal pseudoposition yields interpretable pseudosections. In a VRP survey, the pseudodepth is in many ways analogous to horizontal pseudoposition in a linear surface array as it is in the direction parallel to a line containing the electrodes. However, in a VRP survey, the effect of the ground surface is different from a surface survey. In a VRP survey, current can travel outward from electrodes in any direction until it reaches the ground surface. The presence of the ground surface then causes the pseudodepth to be displaced from the midpoint of the array even for symmetrical arrays.

In surface resistivity surveys, the pseudodepth is usually taken to be either some fraction of the current electrode spacing, or distance between dipole pairs in the case of a dipole-dipole survey, or is calculated based on the median of the sensitivity function for a constant resistivity half space (*Roy and Apparoa*, 1971; *Edwards*, 1977; *Szalai et al.*, 2009). While the depth estimate based on electrode spacing is reasonable for most common surface array types, for irregular arrays of the type that arise with multiple channels the estimate may not be useful. The median depth of the depth sensitivity function works well as a pseudodepth, however, for all surface array types except for pole-pole arrays, there is no simple mathematical formula for the median depth and it must be calculated numerically. *Butler* (2016) showed that the average or mean depth of the depth sensitivity function yields a simple mathematical formula and that its use as a pseudodepth leads to interpretable pseudosections. For VRP surveys, the horizontal pseudoposition is analogous

to the pseudodepth for surface arrays since it is the direction perpendicular to the line through the electrodes. The different geometry of the ground surface again leads to a difference in the formulas for these quantities.

In what follows, I will first derive an expression for the sensitivity function for a half space of constant resistivity for VRP taking into account the effect of the ground surface. I will then use this expression to derive the vertical and horizontal sensitivity functions. Simple expressions for the mean vertical and horizontal positions will then be derived for four electrode arrays. For pole-pole arrays for which the mean value expressions diverge, formulas for calculating the median position are given. In a subsequent section, I will examine the sensitivity functions for a few array geometries. Synthetic depth and horizontal profiles as well as pseudosections calculated with the new pseudoposition formulas will then be presented and I will show that these give results that are superior to those plotted assuming pseudopositions based on averages of the electrode positions or spacings.

2 | THEORY

For simplicity, I consider first the sensitivity for a pole-pole array. Because of the linearity of the governing equations, the sensitivity for general four electrode configurations can be generated by taking linear combinations of sensitivity functions for different electrode combinations. For a pole-pole array, with current electrode A and potential electrode M, the sensitivity of the measured apparent resistivity, ρ_a, to a change in the resistivity in the ground in a subvolume indexed by i is proportional to the dot product of the current densities, $\mathbf{J_A}$ and $\mathbf{J_M}$, of the array and its reciprocal array (*Park and Van*, 1991; *Spitzer*, 1996; *Gomez-Trevino and Esparza*, 2014; *Gomez-Trevino and Flores*, 2015).

$$\frac{d\rho_a}{d\rho_i} = k_{gAM} \frac{\int \mathbf{J_A} \cdot \mathbf{J_M} dV_i}{I_A I_M}. \tag{1}$$

Here, k_{gAM} is the geometerical factor while I_A and I_M are the total currents injected at A and in the reciprocal array at M.

The sensitivity, S_{AM}, to a change in resistivity in an infinitessimal volume at position (x, y, z) can then be seen to be

$$S_{AM}(x, y, z) = k_{gAM} \frac{\mathbf{J_A} \cdot \mathbf{J_M}}{I_A I_M}. \tag{2}$$

I develop the theory for sensitivity of a VRP array placing the horizontal position of the borehole at $x = y = 0$ and using the convention that the z axis is positive down. In a semi-infinite half space with uniform resistivity, ρ, the current density due to injection at electrode A at depth z_A will be given by

$$\mathbf{J_A} = \frac{I_A}{4\pi} \{ \frac{x\hat{i} + y\hat{j} + (z - z_A)\hat{k}}{[(x^2 + y^2 + (z - z_A)^2]^{3/2}} + \frac{x\hat{i} + y\hat{j} + (z + z_A)\hat{k}}{[x^2 + y^2 + (z + z_A)^2]^{3/2}} \}. \tag{3}$$

Here $\hat{i}$, $\hat{j}$ and $\hat{k}$ are unit vectors in the x, y and z directions. The first term on the right represents the effect of a current source in an infinite space while the second term takes into account the effect of an image current at position $(0, 0, -z_A)$ which forces the normal component of the current density to be 0 at the ground surface ($z = 0$). The electrical potential due to electrode A is

$$V_A = \frac{I_A \rho}{4\pi} \{ \frac{1}{[(x^2 + y^2 + (z - z_A)^2]^{1/2}} + \frac{1}{[x^2 + y^2 + (z + z_A)^2]^{1/2}}. \tag{4}$$

From equation 4, the geometrical factor can be shown to be

$$k_{gAM} = 4\pi(|z_M - z_A|^{-1} + |z_M + z_A|^{-1})^{-1}. \tag{5}$$

This is the same form as shown in *Qian et al.* (2007) and *Ali* (2020). Using equation 3 and an analogous form for the current density due to current from electrode M in the reciprocal array in equation 1 we get the sensitivity of a VRP pole-pole array to a small change in resistivity in an infinitesimal volume at point (x, y, z)

$$S_{AM}(x,y,z) = \frac{k_{gAM}}{16\pi^2}\{\frac{x^2+y^2+(z-z_A)(z-z_M)}{[(x^2+y^2+(z-z_A)^2]^{3/2}[(x^2+y^2+(z-z_M)^2]^{3/2}} + \frac{x^2+y^2+(z+z_A)(z-z_M)}{[(x^2+y^2+(z+z_A)^2]^{3/2}[(x^2+y^2+(z-z_M)^2]^{3/2}}$$

$$\frac{x^2+y^2+(z-z_A)(z+z_M)}{[(x^2+y^2+(z-z_A)^2]^{3/2}[(x^2+y^2+(z+z_M)^2]^{3/2}} + \frac{x^2+y^2+(z+z_A)(z+z_M)}{[(x^2+y^2+(z+z_A)^2]^{3/2}[(x^2+y^2+(z+z_M)^2]^{3/2}}\}. \tag{6}$$

The first term in equation 6 gives the sensitivity for a pole-pole array in an infinite space while the subsequent terms represent the effects due to the interactions of the electrodes with the image current sources and of the image currents sources with one another. The first term is typically the dominant one.

For a general four electrode array, consisting of current electrodes A and B and potential electrodes M and N, the total sensitivity, S_4, can be calculated from

$$S_4 = k_{g4}(\frac{S_{AM}}{k_{gAM}} - \frac{S_{AN}}{k_{gAN}} - \frac{S_{BM}}{k_{gBM}} + \frac{S_{BN}}{k_{gBN}}). \tag{7}$$

Here the various pole-pole sensitivity functions and geometrical factors can be determined by making appropriate index substitutions into equations 5 and 6. Note that S_{tot} will consist of the sum of 16 terms. The four electrode geometrical factor is given by

$$k_{g4} = 4\pi(|z_M-z_A|^{-1}+|z_M+z_A|^{-1}-|z_M-z_B|^{-1}-|z_M+z_B|^{-1}-|z_N-z_A|^{-1}-|z_N+z_A|^{-1}+|z_N-z_B|^{-1}+|z_N+z_B|^{-1})^{-1}. \tag{8}$$

2.1 | Vertical Sensitivity

The vertical sensitivity function, $F(z)$, for a pole-pole array, that is the sensitivity of a VRP array to a small change in resistivity in an infinitesimally thin slab with normal in the z direction can be calculated by integrating equation 6 with respect to x and y from $-\infty$ to ∞. This can be carried out by noting the symmetry of equation 6 with respect to a rotation about the borehole axis and so making the substitution $r = \sqrt{x^2+y^2}$ and working in cylindrical coordinates to carry out the integral. This procedure yields

$$F_{AM}(z) = \frac{k_{gAM}}{4\pi}[(2z - z_A - z_M)^{-2}(z < z_- + z > z_+) + (2z - z_A + z_M)^{-2}(z > z_A)$$

$$+(2z + z_A - z_M)^{-2}(z > z_M) + (2z + z_A + z_M)^{-2}]. \tag{9}$$

Here z_- and z_+ are the larger and smaller of z_A and z_M and I take the inequalities to be Boleans equal to 1 when true and 0 when false. The first term in equation 9 represents the vertical sensitivity for two electrodes in an infinite space

and is of the same form as the horizontal sensitivity for a pole-pole array on the ground surface (*Butler*, 2017) differing by only a factor of 2. The remaining three terms represent the effects of the interactions of the A electrode with the image of M, the M electrode with the image of A and the interactions of the two image current sources. Note that equation 9 is discontinous at each of the electrode depths. Note also that $\int_0^\infty F_{AM}(z)dz = 1$ which must be the case since $\frac{d\rho_a}{d\rho_i}$ must be one for homogenous ground.

The vertical sensitivity for a general four electrode array can be constructed from

$$F_4(z) = k_{g4}[\frac{F_{AM}(z)}{k_{gAM}} - \frac{F_{AN}(z)}{k_{gAN}} - \frac{F_{BM}(z)}{k_{gBM}} + \frac{F_{BN}(z)}{k_{gBM}}]. \tag{10}$$

2.2 | Vertical Mean Position

The mean vertical position for a general four electrode array can be calculated from

$$z_{mean} = \int_0^\infty F_4(z)z\,dz, \tag{11}$$

using equation 10 this becomes

$$z_{mean} = \frac{k_{g4}}{4\pi}[\frac{z_A + z_M}{2|z_A - z_M|} - \frac{z_A + z_N}{2|z_A - z_N|} - \frac{z_B + z_M}{2|z_B - z_M|} + \frac{z_B + z_N}{2|z_B - z_N|} + \ln(\frac{(z_A + z_N)(z_B + z_M)}{(z_A + z_M)(z_B + z_N)})]. \tag{12}$$

The first four terms have the same form as the horizontal mean position for a linear surface array (*Butler*, 2017) and are the same as would be seen for current sources in an infinite space. The logarithmic term arises from the image current sources. The form for a pole-dipole array can be easily derived by setting the appropriate electrode position to infinity. Unfortunately, as for the mean depth and mean horizontal position for a surface pole-pole array, the formula for the mean depth of a pole-pole array diverges to infinity logarithmically and so is not a useful formula.

Since equation 12 returns infinity for a pole-pole array, it is recommended to use the median depth as the pseudodepth for these arrays. The median depth, z_{med}, can be calculated by integrating equation 10 from 0 to z_{med} or from z_{med} to ∞ and setting the result equal to 1/2. For a pole-pole array, provided that z_{med} is greater than z_A and z_M this gives

$$(|z_M - z_A|^{-1} + (z_M + z_A)^{-1})^{-1}[(2z_{med} - z_A - z_M)^{-1} + (2z_{med} - z_A + z_M)^{-1}$$

$$+(2z_{med} + z_A - z_M)^{-1} + (2z_{med} + z_A + z_M)^{-1}] = 1. \tag{13}$$

Even for a simple pole-pole array, z_{med} must then be determined numerically for the general case. For the special case of a pole-pole array with either A or M at the ground surface, we have

$$z_{med} = z_+(\frac{1 + \sqrt{2}}{2}). \tag{14}$$

Note that the median depth is actually deeper than either electrode in the pole-pole survey because of the effect of the ground surface.

2.3 | Horizontal Sensitivity

The sensitivity of a VRP survey to a slab of infinitesimal thickness with normal in the x direction extending from $-\infty$ to ∞ in the y direction and from 0 to ∞ in the z direction, $G(x)$, can be calculated by integrating equation 6 over the y and z variables. Each of the terms in equation 6 has the same form as the integral presented in *Roy and Apparoa* (1971) with an exchange of the x and z variables. The only difference is that in the VRP case, z runs from 0 to ∞ while x ranged from $-\infty$ to ∞ for the surface survey. While each term in equation 6 is not symmetric about $z = 0$, the sum of the terms is symmetric about $z = 0$ because of the placement of the image currents and so the integral can be computed by integrating z from $-\infty$ to ∞ and dividing by 2. This procedure yields

$$G_{AM}(x) = \frac{k_{gAM}|x|}{2\pi}\{[(z_A - z_M)^2 + 4x^2]^{-3/2} + [(z_A + z_M)^2 + 4x^2]^{-3/2}.\} \tag{15}$$

This is the same form as the depth sensitivity function first derived by *Roy and Apparoa* (1971) and the later sensitivity of a linear surface array (*Butler*, 2017) up to multiplicative constants.

The sensitivity function for a general four electrode array is then

$$G_4(x) = k_{g4}(\frac{G_{AM}(x)}{k_{gAM}} - \frac{G_{AN}(x)}{k_{gAN}} - \frac{G_{BM}(x)}{k_{gBM}} + \frac{G_{BN}(x)}{k_{gBN}}), \tag{16}$$

where again the various G_{ij} functions can be derived by substituting the appropriate indices into equation 15. Note that the choice of orientation of the x and y axes is arbitrary and so equation 16 gives the sensitivity in any direction.

2.4 | Mean Horizontal Distance

The mean of the horizontal sensitivity for a four electrode array can be calculated from

$$x_{mean0} = \int_{-\infty}^{\infty} G_4(x)x\,dx.$$

Since $G_4(x)$ is an even function in x, directly evaluating equation 2.4 results in $x_{mean0} = 0$. In order to get a measure of the extent to which sensitivity extends outward from the borehole, we can instead integrate over the absolute value of x or alternatively, consider the average of x weighted by the sensitivity on only one side of the borehole.

$$x_{mean} = \int_{-\infty}^{\infty} G_4(x)|x|dx = \frac{\int_0^{\infty} G_4(x)x\,dx}{\int_0^{\infty} G_4(x)dx}. \tag{17}$$

Evaluating this integral gives a form very similar to the mean depth for a surface array derived by *Butler* (2016) except that there are contributions from the image current source. For a general four electrode array we have

$$x_{mean} = \frac{k_{g4}}{8\pi}\ln(\frac{|z_A - z_N||z_A + z_N||z_B - z_M||z_B + z_M|}{|z_A + z_M||z_A - z_M||z_B - z_N||z_B + z_N|}). \tag{18}$$

Note that a VRP is equally sensitive to resistivity variations in all horizontal directions and so x_{mean} gives an indication of the horizontal distance from a borehole over which a measurement is sensitive but gives no information about the direction.

The mean horizontal sensitivity can be calculated for a pole-dipole array from equation 18 by setting the z position of one of the electrodes to infinity. Equation 18 diverges for a pole-pole array so for these arrays another horizontal estimate is used and it is suggested to use the horizontal median.

For a pole-pole array, the horizontal median for $x > 0$ can be determined by integrating equation 15 from 0 to ∞ and setting the result equal to 1/4. This procedure results in the following equation that must be solved numerically for x_{med}.

$$(|z_A - z_M|^{-1} + (z_M + z_A)^{-1})^{-1}\left(\frac{1}{\sqrt{(z_A - z_M)^2 + 4x_{med}^2}} + \frac{1}{\sqrt{(z_A + z_M)^2 + 4x_{med}^2}}\right) = \frac{1}{2}. \tag{19}$$

For the special case with either electrode at $z = 0$ this can be shown to give

$$x_{med} = \frac{\sqrt{3}}{2} z_+. \tag{20}$$

3 | RESULTS

3.1 | Sensitivity

Figure 1a displays the radial sensitivity as a function of depth and radial distance from the borehole for a pole-pole array with electrodes at depths 1 and 5. The plot begins at radius 0.4 to avoid infinite values on the borehole axis. For comparison, the sensitivity for a surface array (*Barker*, 1989) with electrodes at $x = 1$ and $x = 5$ is shown in figure 1b. The overall shape for the VRP sensitivity is similar to that for a surface array rotated by 90° with sensitivity dipoles in the vicinities of the two electrodes. There is a region with negative sensitivity between the two electrodes where the current densities from the A and M electrodes are flowing in opposite directions and positive regions outside where the current densities are flowing in the same directions. Note that in the borehole array, the sensitivity dipole associated with the upper electrode is reduced in strength because of the effects of the surface boundary that are incorporated in these calculations through the image current sources. Note that the sensitivity for the VRP is symmetric to a rotation about the borehole axis. Sensitivity functions for other array types are also similar to those for surface arrays rotated by 90° but the function near the surface is affected by the boundary if the depth to the array is small or similar to the depth to the array.

3.2 | Vertical Sensitivity

Figure 2a) shows $F(z)$ as calculated from equation 10 for a pole-pole array ($z_M = 1$, $z_A = 5$), a pole-dipole array ($z_M = 1$, $z_N = 2$, $z_A = 5$), and a dipole-dipole arrray ($z_M = 1$, $z_N = 2$, $z_A = 5$, $z_B = 6$). The formula was verified by carrying out numerical simulations using Comsol Multiphysics (*Butler and Sinha*, 2012; *Butler and Zhang*, 2016) with and without the effects of a slab with z normal with resistivity $1.01 \times \rho_0$ where ρ_0 was the background resistivity. The vertical sensitivity was then calculated as $F(z) \approx (\rho_{a1} - \rho_{a0})/(0.01h)$ where ρ_{a1} and ρ_{a0} were the apparent resistivities calculated with and without the effect of the slab and h was the thickness of the slab (taken to be 0.5). As can be seen, the agreement between the sensitivitiy functions calculated numerically and from equation 10 is excellent. Asterisks show the positions of z_{mean} as calculated from equation 12 for the pole-dipole array and the dipole-dipole arrray and of z_{med} as calculated from equation 13 for the pole-pole array. The discontinuities in sensitivity at the electrode positions can be clearly seen.

The sensitivity of the dipole-dipole array to a slab is dominantly within the two dipoles. For a surface pole-pole array, the horizontal sensitivity is 0 between the electrodes (*Butler*, 2017) while it is slightly greater than 0 in a VRP due to the effect of the surface boundary. The lower amplitude of the pole-pole sensitivity in figure 2a) indicates that there is greater sensitivity at depth beyond the region plotted for similar electrode positions for the pole-pole array.

For the pole-pole array, z_{med} is slightly deeper than the deeper electrode. For the pole-dipole array, z_{mean} is close to the pole of the array while for the dipole-dipole array, z_{mean} is slightly deeper than the midpoint of the array due to the effects of the surface boundary.

3.3 | Horizontal Sensitivity

Equation 16 is used to plot the horizontal sensitivity for the same arrays as shown in figure 2a). The horizontal sensitivity was also calculated from numerical simulations in the same manner as described in section 3.2 except that the slabs had normal in the x direction. Again, the agreement between the sensitivitiy functions calculated numerically and from equation 16 is excellent. Asterisks indicate x_{mean} as calculated from equation 18 for the pole-dipole and dipole-dipole arrays and x_{med} for the pole-pole array as calculated from equation 19. Unlike the vertical sensitivity, the horizontal sensitivity varies smoothly. It can be seen that the sensitivity of the pole-pole array (blue) extends significantly farther from the borehole axis than either the dipole-dipole or pole-dipole arrays.

4 | SYNTHETIC EXAMPLES

4.1 | Vertical Profiles

In order to test the use of z_{mean} as calculated from equation 12 as pseudodepth, additional simulations were carried out using the finite element modeling package Comsol Multiphyics. Two two-layer scenarios with a boundary at $z = 10$ m were investigated. The resistivity in the model was set to 10 Ωm and 1 Ωm in the upper and lower regions for the models whose results are displayed in figure 3 parts a) and b) and 1 Ωm and 10 Ωm for the models whose results are shown in parts c) and d). In order to consider all possible array types, including highly asymmetric ones that might result from multichannel potential measurements, four electrode arrays were constructed by randomly choosing positions of the electrodes between 0 and 45 m depth with equal numbers of arrays with 0,1,2,3 and 4 electrodes in the lower region. The resulting apparent resistivity values are plotted vs z_{mean} in figure 3 a) and c). For comparison with a more conventional choice for the pseudodepth, apparent resistivity is plotted vs z_{av} (the average of the four electrode positions) in parts b) and d). Note that z_{av} gives the mid-point for frequently used symmetrical four electrode arrays such as Wenner, dipole-dipole and pole-pole arrays. A total of 1447 points are plotted for both sets of simulations and an additional 11 simulations produced results with apparent resistivity significantly greater than 15 that are not shown. As can be seen, both choices for pseudodepth result in reasonable vertical profiles, albeit with significant scatter. The apparent resistivity vs pseudodepth plots conform better to the actual resistivity profile (plotted in red) for the case with a resistive upper layer.

Comparing the plots of apparent resistivity with pseudodepth plotted with z_{mean} with those plotted with z_{av}, it can be seen that apparent resistivity values intermediate between the actual resistivities of the upper and lower layers plot more closely to 10 m depth (the actual depth of the interface) when plotted with z_{mean} (especially for the simulations with the resistive surface layer) while there is greater scatter when plotted with z_{av}. The RMS missfits between the apparent resistivity profiles with pseudodepth and the actual resistivity profiles are 4.6 and 4.1 (for the resistive and conductive upper layer cases) when plotted with z_{mean} while they are 7.6 and 6.5 when plotted with z_{av}

indicating greater agreement with the actual resistivity profiles when z_{mean} is used as the pseudodepth.

4.2 | Horizontal Profiles

I next test the utility of plotting horizontal profiles using x_{mean} as calculated from equation 18 as the horizontal pseudoposition. For comparison, I also show profiles plotted using Δz_{max} (the maximum distance between electrodes) as an estimate of the horizontal pseudoposition. A series of simulations were carried out with a step in resistivity at position $x = 5$ m from 1 to 10 Ωm with increasing x (figure 4 a and b) and from 10 to 1 (figure 4 c and d). For values of $x < 0$ the resistivity was taken to be the same as its value between $x = 0$ and $x = 5$. In each case 1489 simulations were carried out with randomly chosen electrode positions . A small number of results are not plotted because the results are off the diagram.

For these simulations, the apparent resistivity varies only weakly, because the resistive anomaly exists only on one side while the current can flow out of the borehole in all directions. Comparing the plots using x_{mean} as the horizontal pseudoposition with those using Δz_{max}, it can be seen that plots using x_{mean} exhibit significantly less scatter and are closer to monotonically varying functions. The profiles plotted with x_{mean} start to show variation from the near-borehole resistivity only for values of x_{mean} that are significantly greater than the actual value at which the resistivity in the ground changes and so x_{mean} is not seen to be good for determining the actual position of the resistivity step. The choice of Δz_{max} for the comparison plot was arbitrary and a fraction of this value could have been chosen instead which would have more closely conformed to the profile of the actual resistivity in the ground near the borehole. Overall, the profiles plotted with x_{mean} are deemed to be superior because of the lower scatter and their near monotonicity.

4.3 | Vertical and Radial Variations

Simulations of VRP with randomly generated electrode positions were undertaken in which a rectangular prism with square cross section of side length 10 m of different resistivity from the background was introduced with top left corner at position $x = 5$m, $z = 5$m. The results of the simulations are shown as scatter-plot pseudosections in figure 5. In figures 5a) and b) , the background resistivity was 10 Ωm while the resistivity inside the prism was 1 Ωm while in figures 5c) and d) the resistivity values were reversed. In both cases, the changes in the apparent resistivity from the background values were small because the block was only on one side of the borehole. Values were binned according to the thresholds shown in the legend. The pseudosections plotted using x_{mean} as the pseudoposition are clearly more spread out than those plotted with Δz_{max}. However, the use of z_{mean} and x_{mean} as the pseudopositions clearly sorts the data more coherently and there is a recognizable low in resistivity in figure 5a) and a high in figure 5c). However, the largest variations in resistivity (green asterisks) plot somewhat to the right of the actual anomalous region and some of the green points do not plot with the main cluster. Trends are significantly less apparent for data plotted with z_{av} and Δz_{max} (figures 5c and d) and it would be more difficult to discern a high or a low based on these pseudosections.

5 | CONCLUSIONS

The sensitivity function for a VRP in constant resistivity ground has been been derived and presented. Expressions for the vertical and horizontal sensitivity functions have also been derived as well as expressions for the horizontal (equation 18) and vertical means (equation 12). Mean values do not converge for pole-pole arrays and so it is recommended

to use the median value instead and expressions to be evaluated numerically for the vertical and horizontal median are presented. Results for synthetic VRP surveys are presented with x_{mean} and z_{mean} used as the pseudopositions and these are shown to be more readily interpreted than pseudosections plotted with the average electrode depth and array length as the pseudodepth and pseudoposition as they separate the high and low values more coherently.

Here, I have concentrated on VRP arrays because the vertical and horizontal sensitivity functions and mean values admit simple mathematical formulas. For borehole-borehole surveys, surface to borehole or borehole surveys where the borehole is not close to vertical, equation 7 could be multiplied by x and integrated over the lower half-space numerically to obtain x_{mean} and a similar procedure could be used to find z_{mean}.

I expect that the formulas presented here for x_{mean} and z_{mean} will be useful for plotting pseudosections from VRP data. The formulas also give simple estimates of the sensitivity distances and so will be useful for survey planning and initial interpretation.

references

Ali, M., Sun, S., Qian W., Bohari A. D., Claire D.,Faruwa A.R.,and Zhang Y., 2020, Borehole resistivity and induced polarization tomography at the Canadian Shield for Mineral Exploration in north-western Sudbury, *E3S Web of Conferences 168*, https://doi.org/10.1051/e3sconf/202016800002.

Banerjee, B., Pal, B.P., 1986, Lateral response functions for different linear configurations in resistivity methods for a homogeneous half-space. *Explor. Geophys.*, **17**, 87–92.

Barker, R.D., 1989. Signal contribution sections and their use in resistivity studies. *Geophys. J. R. Astro. Soc.* **39**, 123–129

Bhattacharya B.B, and Shalivahan S. 2016. *Geoelectric Methods: Theory and Application*. McGraw Hill Education (India).

Butler, S.L. (2021). Data Sets and Code for Simple formulas for pseudoposition for electrical resistivity and IP in vertical boreholes based on mean positions of the sensistivity (Version 1) . Zenodo. http://doi.org/10.5281/zenodo.4975634

Butler, S.L., 2017, Analysis of the moments of the sensitivity function for resistivity over ahomogeneous half-space: Rules of thumb for pseudoposition, offlinesensitivity and resolution, *J. App. Geophys.*, **143**, 149-155.

Butler, S.L., 2016. The mean sensitivity depth of the electrical resistivity method. *Geophys. Prosp.*, **64**, 1399–1409. http://dx.doi.org/10.1111/1365-2478.12354.

Butler, S.L., Zhang, Z., 2016. Forward modeling of geophysical electromagnetic meth-ods using Comsol. *Comp. Geosci.*, **87** http://dx.doi.org/10.1016/j.cageo.2015.11.004.

Butler, S.L., Sinha, G., 2012. Forward modeling of applied geophysics methods using Comsol and comparison with analytical and laboratory analog models. *Comp. Geos.*, **42**, 168–176. http://dx.doi.org/10.1016/j.cageo.2011.08.022.

COMSOL Multiphysics® v. 5.6. www.comsol.com. COMSOL AB, Stockholm, Sweden.

Daniels, J.J. and Van Dyck, A., 1984. Borehole Resistivity and Electromagnetic Methods Applied to Mineral Exploration, *IEEE Transactions on Geoscience and Remote Sensing*, **GE22.**, 80-87.

Denis, A., Marache, A., Obellianne, T., Breysse, D., 2002,Electrical resistivity borehole measurements:application to an urban tunnel site, *J. App. Geophys.*, **50**, 319–331.

Edwards, L.S., 1977. A modified pseudosection for resistivity and induced-polarization, *Geophysics*, **42**, 1020-1036.

Gómez-Treviño, E., Esparza, F.J., 2014. What is the depth of investigation of a resistivity measurement? *Geophysics*, **79**, W1–W10.http://dx.doi.org/10.1190/GEO2013-0261.1.

Gómez-Treviño, E., Flores, C., 2015. Alternative theory for signal contribution sectionsand depth of investigation characteristics in electrical prospecting. *Geophys.Prosp.* **63**, 740–749.http://dx.doi.org/10.1111/1365-2478.12214

Loke M.H., Chambers, J.E., Rucker, D.F., Kuras, O., and Wilkinson P. 2013. Recent developments in the direct-current geoelectrical imaging method, *J. App. Geophys.*, **95**, 135-156.

Park S.K. and G.P. Van, 1991, Inversion of pole-pole data for 3-D resistivity structure beneath arrays of electrodes, *Geophysics*, **56**, 951-960.

Qian, W., Milkereit, B., McDowell, G., Stevens, K., Halladay, S. 2007. Borehole Resistivity Logging and Tomography for Mineral Exploration, in "Proceedings of Exploration 07: Fifth Decennial International Conference on Mineral Exploration" edited by B. Milkereit, 1115-1118.

Roy A. and A. Apparoa, 1971. Depth of investigation in direct current methods, *Geophysics*, **36**, 943-959.

Reynolds, J.M., 2011. An Introduction to Applied and Environmental Geophysics, 2nd Edition, Wiley.

Spies, B.R. 1996. Electrical and electromagnetic borehole measurements: A review, *SURVEYS IN GEOPHYSICS*, **17**, 517-556.

Spitzer, K., 1998, The three-dimensional DC sensitivity for surface and subsurface sources, *Geophys. J. Int.*, **134**, 736-746.

Szalai, S., Novák, A., Szarka, L., 2009. Depth of investigation and vertical resolution ofsurface geoelectric arrays. *J. Environ. Eng. Geophys.*, **14**, 15–23. http://dx.doi.org/10.2113/JEEG14.1.15.

acknowledgements

This work was funded by the National Sciences and Engineering Research Council of Canada.

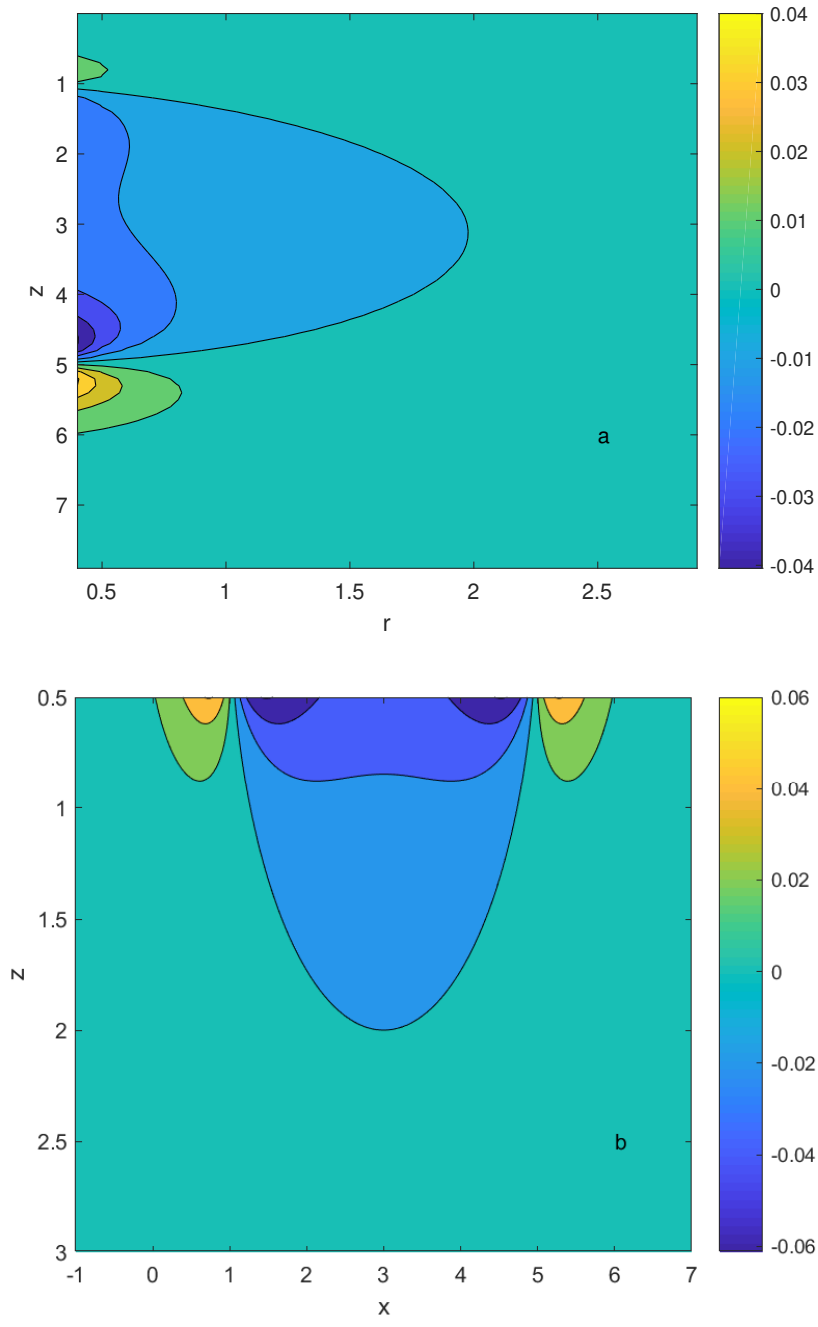

FIGURE 1 a) The radial sensitivity for a pole-pole array with electrodes at $z = 1$ and 5 as calculated from equation 6. b) The sensitivity for a surface pole-pole array with electrodes at positions 1 and 5.

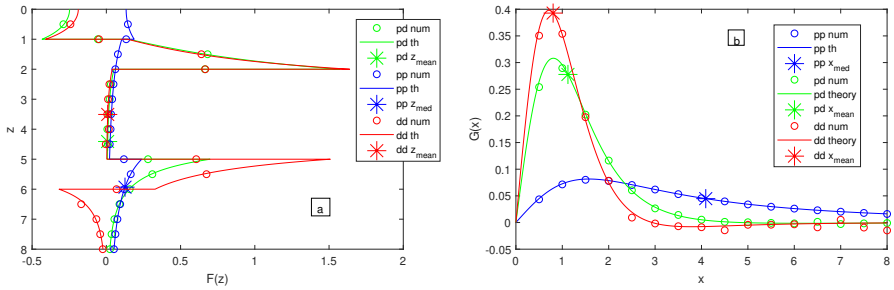

FIGURE 2 Vertical a) and horizontal b) sensitivity as calculated from equations 10 a) and 16 b) (solid lines, labeled th) for a pole-pole array ($z_M = 1$, $z_A = 5$, blue, labeled pp), a pole-dipole array ($z_M = 1$, $z_N = 2$, $z_A = 5$, green, labeled pd) and a dipole-dipole array ($z_M = 1$, $z_N = 2$, $z_A = 5$ and $z_B = 6$, red, labeled dd). Circles show values determined from numerical simulations (num). Asterisks show z_{mean} and x_{mean} as calculated from equations 12 and 18 for the pole-dipole and dipole-dipole arrays and show z_{med} and x_{med} as calculated from equations 13 and 19 for the pole-pole array.

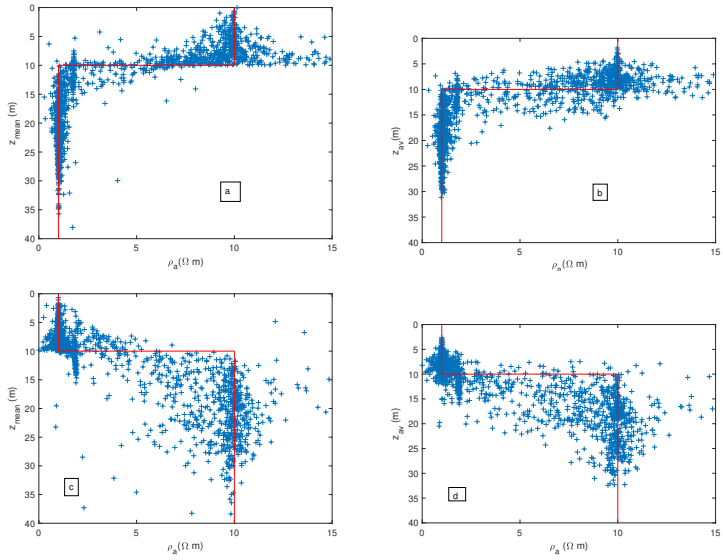

FIGURE 3 Vertical profiles of apparent resistivity across a step resistivity contrast for a synthetic VRP survey. Positions of A, B, M and N electrodes were randomly generated with values between 0 and 45. Apparent resistivity is plotted against z_{mean} in parts a) and c) and z_{av} in parts b) and d). The true resistivity is plotted in red.

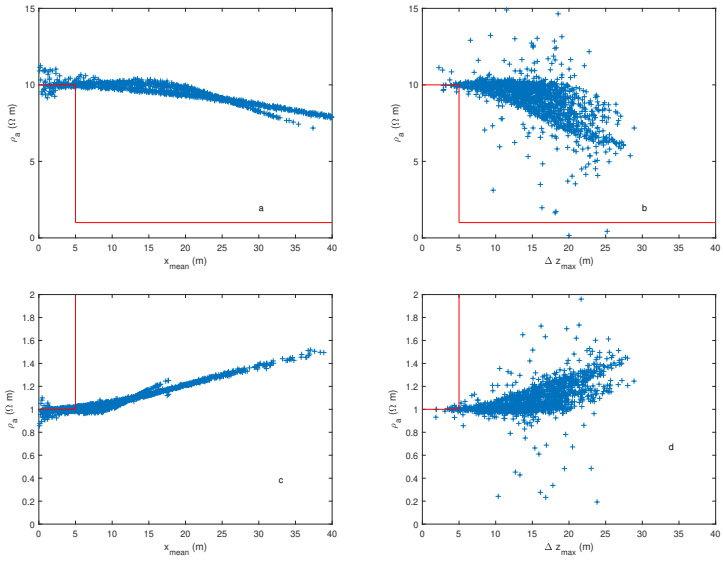

FIGURE 4 Horizontal profiles of apparent resistivity across a step resistivity contrast for a synthetic VRP survey. Positions of *A*, *B*, *M* and *N* electrodes were randomly generated with values between 0 and 45. Apparent resistivity is plotted against x_{mean} in parts a) and c) and Δz_{max} in parts b) and d). The true resistivity is plotted in red (for parts c and d the true resistivity goes to 10 for $x > 5$.)

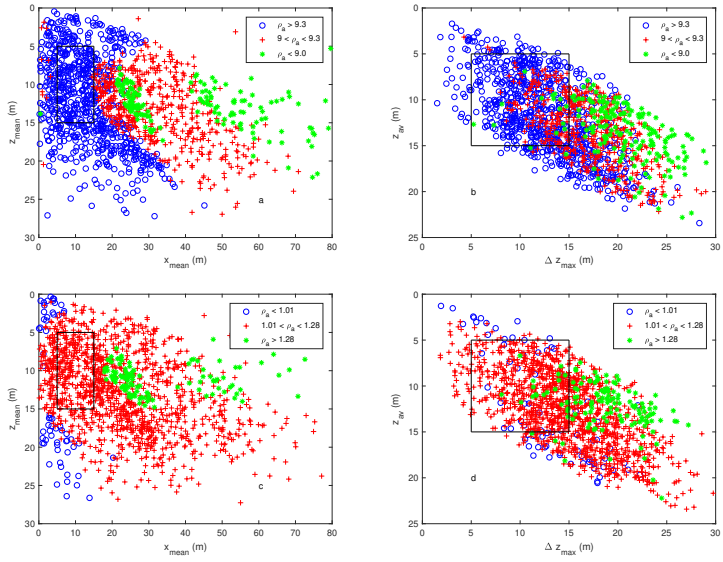

FIGURE 5 Pseudosections ofthe results of simulations using randomly generated arrays. Resistivity is constant except for constant resistivity within a horizontal rectangular prism. A slice through the prism in the $x - z$ plane is shown as the black square. In a) and b) the background resistivity was 10 Ωm while the resistivity inside the block was 1 while in c) and d) the resistivity outside the block was 1 and inside it was 10. The data points have been grouped into the bins indicated in the legend.